A Nonisolated Transformerless High Voltage Gain Buck Boost dc-dc Converter

Mohammad Reza Banaei[1], Hossein Ajdar Faeghi bonab[2*]

***Abstract*—A novel transformer less high step-up buck–boost dc-dc converter is proposed in this paper. The output voltages of some sources such as fuel cell, photovoltaic are not regulated. Therefore voltage regulation is required to fix the DC-link voltage. Hence, a buck boost DC/DC converter is suitable to regulate the output voltage of these sources. The presented converter voltage gain is higher that of the conventional boost, buck boost, CUK, SEPIC and ZETA converters and high voltage gain can be obtained with a suitable duty cycle. In this converter, only one power switch is utilized. The voltage stress across the power switch and diodes is low. Hence, the low on-state resistance of the power switch can be selected to decrease conduction loss of the switch and improve efficiency. The low voltage stress across the diodes allows the prevent the reverse-recovery current problem. The proposed converter can be operated in the continuous conduction mode (CCM) and the discontinuous conduction mode (DCM). The presented converter has simple structure; therefore the control of the proposed converter will be easy. The principle of operation and the mathematical analyses of the proposed converter are explained. The validity of the presented converter is verified by the experimental results.**

***Index Terms*— Buck boost dc-dc converter; voltage gain; duty cycle, voltage stress..**

I. INTRODUCTION

In recent years, environmental troubles, such as climate or change and global warming by increased emissions of carbon dioxide, are very important. With increasing attention to environmental problems, energy achieved from the fuel cell systems is focused on the low environmental effects and clean energy. Fuel cells are an effective alternative to replace fuels in emergency power systems and vehicles. Fuel cells can be used as clean energy by users with low emissions of carbon dioxide. Due to steady operation with renewable fuel supply and high effectiveness and efficiency, the fuel cell has been recognized increasingly as a suitable alternative source. There are some problems of this fuel such as high costs, but they have brilliant features such as high efficiency and small size. Due to this explanation, the fuel cell is appropriate as power supplies for telecom back-up facilities and hybrid electric vehicles. The output voltage of the fuel cell unit cell is low and is not steady and it cannot be directly connected to the load. For applications that need a steady DC voltage, buck-boost dc-dc converter is required [1-5]. However, the traditional buck-boost converter is not suitable for fuel cells sources. The traditional buck-boost converter efficiency is expected high; however, it is low and is

Nomenclature	
r_{DS}	Switch on-state resistance
R_{F1} and R_{F2}	Diodes D_1 and D_2 forward resistances
V_{F1} and V_{F2}	Diodes D_1 and D_2 threshold voltages
R_{L1} and R_{L2}	ESR of inductors L_1 and L_2
r_{C1}, r_{C2} and r_{C3}	ESR of capacitors C_1, C_2 and C_3
ΔV_{C1}	Voltage ripple of the capacitor C_1
$\Delta V_{C1,ESR}$	Voltage ripple on capacitor C_1 created from the current that flows through the equivalent series resistance
$\Delta V_{C1,cap}$	Voltage ripple of capacitor C_1 created from the charging and discharging
$\tan\delta_{C1}$	Dissipation factor of capacitor C_1
ΔV_{C2}	Voltage ripple of the capacitors C_2
$\Delta V_{C2,ESR}$	Voltage ripple on capacitors C_2 created from the current that flows through the equivalent series resistance
$\Delta V_{C2,cap}$	Voltage ripple of the capacitors C_2 created from the charging and discharging
$\tan\delta_{C2}$	Dissipation factor of capacitors C_2
ΔV_{C3}	Voltage ripple of the capacitors C_3
$\Delta V_{C3,ESR}$	Voltage ripple on capacitors C_3 created from the current that flows through the equivalent series resistance
$\Delta V_{C3,cap}$	Voltage ripple of the capacitors C_3 created from the charging and discharging
$\tan\delta_{C3}$	Dissipation factor of capacitor C_3

Although the flyback converter can obtain the high step-up voltage gain, the power switches suffer a voltage spike across the switches and the converter efficiency is not high because of the reverse-recovery problems and leakage inductor [9-11]. In [12-13] high voltage gain dc-dc converters with a coupled-inductor is proposed. The leakage inductance of the coupled inductor is so important that it cause high voltage spikes and adds the voltage stress. In [14] the switched capacitor method is used to obtain high step up voltage gain. In [15] a high step-up bidirectional dc-dc converter with low voltage stress on the

Manuscript received April 28, 2016; accepted October 22, 2016

[1]Electrical Engineering Department, Azarbaijan Shahid Madani University, Tabriz, Iran, Email: m.banaei@azaruniv.edu
[2]Electrical Engineering Department, Azarbaijan Shahid Madani University, Tabriz, Iran, Email: h.ajdarfaeghi@azaruniv.edu

switch is proposed. In [16-17] transformer less high step-up dc-dc converters are proposed. In [18-19] a transformer less buck-boost dc-dc converter is proposed. The voltage gain for this converter is twice as large as the conventional buck boost converter. In [20] a transformer less interleaved high step-down converter is proposed, but, in the presented converter, two power switches have been utilized and the capacitors of the converter are suddenly charged. In [21] a buck–boost converter based on KY converter is proposed. In this converter, two main switches are used and the voltage gain of the presented converter is 2D. In [22] a multi-output buck boost DC/DC converter is proposed. This converter has several output voltages, but, in the presented converter, many power switches have been used. In [23] a two-stage invertring buck-boost converter is proposed. The presented converter is constructed of two parallel conventional buck-boost converters. In [24] a two-stage buck-boost converter for power factor correction is presented and this converter does not require additional power switch. In [25] a multi-input DC-DC converter is proposed to connect two power sources with a DC bus or load. The presented converter has high efficiency due to obtaining turn-on zero voltage switching (ZVS) of power switches. However, it requires a bidirectional port. In [26] a multi-port bidirectional DC-DC converter is proposed for DC micro grid. An integrated three phase transformer is utilized to enhance the voltage level and isolate low voltage side and high voltage side; therefore, the number of power switches is high hence, two input sources require to share a common ground. In [27] a non-inverting buck–boost converter for fuel-cell system using three power switches is proposed with a voltage gain equal to the proposed converter in this paper. In [28] the high step-up converters, based on coupled inductors to extend voltage gains by adjusting the turns ratios of coupled inductors, are presented. However, the use of coupled inductors would lead to some problems in leakage inductance and pulsating input current. In [29] the transformer less converters are presented. Although the converters do not use coupled inductors, there are too many components, which result in complexity. In [30] an interleaved high step-up converter is presented. The presented converter combines an interleaved boost converter, a voltage multiplier and a cascade three-level boost converter. In this converter, the interleaved boost converter is used to reduce the input current ripple, and the voltage multiplier and the three-level boost converter are used not only to upgrade the voltage gain but also to make the voltage stresses of semiconductors lower than the output voltage. In [31] the interleaved converters with coupled inductors are presented. However, additional active clamp and passive clamp circuits are adopted to reduce the spike voltages across the active switches, and this would result in complicated structure. In [32] a transformerless high voltage gain dc-dc converter, is proposed. the presented converter is consisted of two inductors and two active switches which share the same operation signal and the topology of the converter is very simple. In this paper, a novel single switch transformerless buck boost dc-dc converter with high step-up voltage gain and low voltage stress on the power switch is proposed. The voltage transfer gain of the proposed converter is higher than the classic buck-boost converter, SEPIC, CUK and ZETA converters. The structure of the proposed converter is simple, hence the control of the converter will be easy. In this topology, only one power switch is used which makes the control scheme simple as well as reducing the switching power losses. Moreover, CCM operational region is broadened in the proposed converter in comparison with the converter the voltage stress across the active power switch is reduced which enables the use of MOSFETs with a lower voltage rating and low $R_{DS\text{-}ON}$. Thus, the conversion efficiency can be improved due to the reduced conduction and switching losses. Similarly, the reduced voltage stress across all the diodes in the circuit allows the use of Schottky rectifiers for alleviating the reverse-recovery current problem, leading to a further reduction in the switching losses. The proposed buck-boost converter is utilized in many applications like fuel-cell systems, car electronic devices, LED drivers and gadgets such as mobile phones and notebooks. In this paper, the mathematical analyses of the proposed converter are explained. Besides, to verify the feasibility of the converter, experimental results are provided.

II. OPERATING PRINCIPLE OF THE PROPOSED CONVERTER

The proposed converter is shown in Fig. 1(a). This converter consists one power switch S , two diodes D_1 and D_2, two inductors L_1 and L_2, three capacitors C_1, C_2 and C_3 and load R. In this paper, duty cycle is denoted by D, the switching and time frequency are denoted by F_S and T_S, respectively, the input voltage is signified by Vi, the output voltage is represented by V_o, the voltages across the capacitors C_1, C_2 and C_3 are indicated by, V_{C1}, V_{C2} and V_{C3}, respectively, the voltage across the inductors L_1 and L_2 are signified by V_{L1} and V_{L2}, respectively and the output current is denoted by I_o .

For simplicity of the analysis of the operating principles, the following assumptions are considered:

1) The capacitors of the presented converter are large enough, hence the voltage across capacitors are assumed to be constant.

2) The main switch of the proposed converter is treated as ideal and the parasitic capacitor of the main switch is neglected.

The presented converter can be operated in both the continuous conduction mode (CCM) and the discontinuous conduction mode (DCM). The continuous conduction mode can be divided into two operation modes. The analysis of the presented converter in one switching period under continuous condition mode (CCM) is explained in detail asfollows:1) First mode $\left[0 \le t \le DT_s\right]$: During this time interval as shown in Fig. 1(b), the switch S is turned on and the diodes D_1 and D_2 are turned off. The inductors L_1 and L_2 are magnetized linearly and energy storage in capacitor C_3 is discharged to capacitor C_1 and the capacitor C_2 is discharged. Thus, the relevant equations are found to be:

$$V_{L1} = V_i \tag{1}$$

$$V_{L2} = V_i + V_{C3} - V_{C1} \tag{2}$$

Second mode $[DT_s \le t \le T_s]$: The equivalent circuit is shown in Fig. 1(c). During this time interval, the switch S is turned off and the diodes D_1 and D_2 are turned on. The inductors L_1 and L_2 are demagnetized linearly. The capacitor C_2 is charged by the inductor L_1. The capacitor C_3 is charged by the inductor L_2 and the capacitor C_1 is discharged. The associated equations are found to be:

$$V_{L1} = -V_{C3} \quad (3)$$

$$V_{L2} = -V_{C1} = -V_{C2} \quad (4)$$

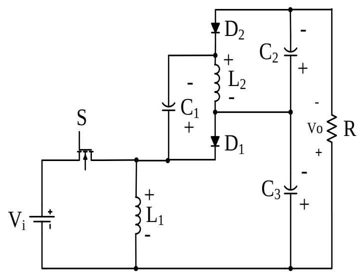

(a)

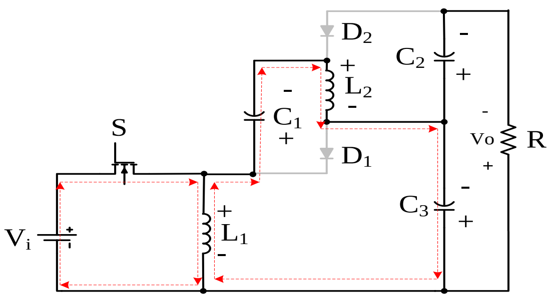

(b)

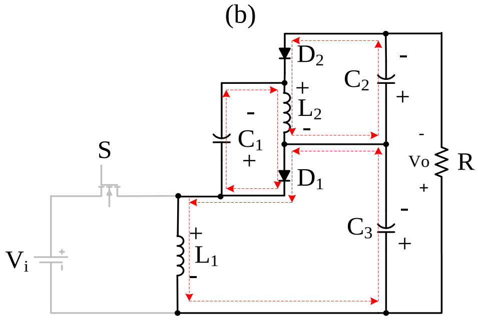

(c)

Fig. 1. (a) Equivalent circuit of the proposed converter (b) mode 1; (c) mode 2.

The voltage gain curves for the proposed converter, conventional boost, buck boost and CUK converters. It is seen that the proposed converter is buck boost and the voltage transfer gain of the converter is higher than that of the other converters.

A. Voltage gain

By applying volt-sec balance principle on the inductor L_1 and using (1) and (3), we have:

$$\int_0^{DT_s} V_i dt + \int_{DT_s}^{T_s} (-V_{C3}) dt = 0 \quad (5)$$

By simplify (5), the voltage across capacitor C_3 (V_{C3}) can be achieved as follows:

$$V_{C3} = \frac{DV_i}{1-D} \quad (6)$$

By applying volt-sec balance principle on the inductor L_1 and using (2) and (4), we have:

$$\int_0^{DT_s} (V_i + V_{C3} - V_{C1}) dt + \int_{DT_s}^{T_s} -V_{C2} dt = 0 \quad (7)$$

By simplify (7), the voltage across capacitor C_2 (V_{C2}) can be obtained as follows:

$$V_{C2} = \frac{DV_i}{1-D} \quad (8)$$

Using (6) and (8), the voltage transfer gain (M_{CCM}) can be achieved as follows:

$$M_{CCM} = \frac{V_o}{V_i} = \frac{V_{C2} + V_{C3}}{V_i} = \frac{2D}{1-D} \quad (9)$$

According to (9), the voltage gain of the proposed converter is higher than that of the conventional boost, buck boost, CUK, SEPIC and ZETA converters and is twice as large as the voltage gain of the conventional buck boost converter.

Fig.2. Shows some typical key waveforms of the proposed converter in continuous conduction mode (CCM).

The voltage gain curves for the proposed converter and conventional boost and buck boost converter are shown in Fig. 3. It is seen that the voltage gain of the proposed converter is higher than the other converters.

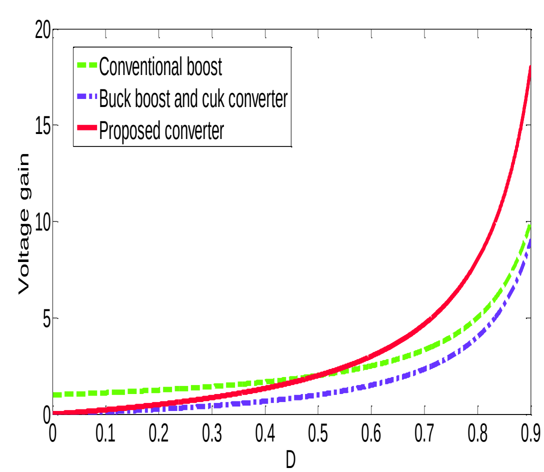

Fig. 2. Curves of voltage gain comparison of proposed converter and other converters at CCM operation.

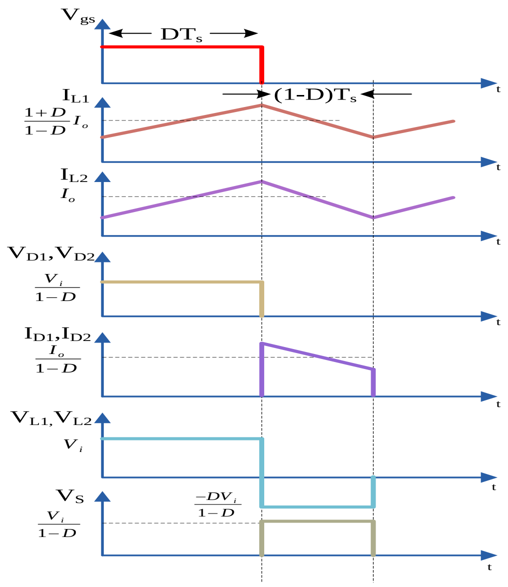

Fig. 3 Key waveforms of the proposed converter at CCM operation

B. Calculation of the currents

The current that flows through the capacitor C_2 during switch on period $(I_{C2,on})$ can be achieved as follows:

$$I_{C2,on} = -I_o \tag{10}$$

The current that flows through the capacitor C_1 during switch on period $(I_{C1,on})$ can be earned as follows:

$$I_{C1,on} = I_{L2} \tag{11}$$

The current that flows through the capacitor C_1 during switch off period $(I_{C1,off})$ can be achieved as follows:

$$I_{C1,off} = I_{L2} - I_{C2,off} - I_o \tag{12}$$

Where, $I_{C2,off}$ is the current that flows through the capacitor C_2 during switch off period.

By applying current-sec balance principle on capacitor C_1, the following equation can be earned as follows:

$$\int_0^{DT} I_{C1,on} dt + \int_{DT}^{T} I_{C1,off} dt = 0 \tag{13}$$

By substituting (10), (11) and (12) into (13), the currents that flow through the capacitor C_1 and the inductor L_2 (I_{L2}) can be obtained as follows:

$$I_{C1,on} = I_{L2} = I_o \tag{14}$$

From Fig. 1(b), the current that flows through the capacitor C_2 during switch on cycle $(I_{C3,on})$ can be achieved as follows:

$$I_{C3,on} = I_{C2,on} - I_{C1,on} = -2I_o \tag{15}$$

According to Fig. 1(c), the current that flows through the inductor L_1 (I_{L1}) can be earned as follows:

$$I_{L1} = (I_{C3} + I_{L2} - I_{C1} - I_{C2})_{off} = \frac{1+D}{1-D} I_o \tag{16}$$

The average of input current (I_i) can be achieved as follows:

$$I_i = \frac{1}{T_s}\left[\int_0^{DT_s} (I_{L1} - I_{C1,on}) dt\right] = \frac{2D}{1-D} I_o \tag{17}$$

According to Fig. 1(b), the current that flows through the switch S (I_S) can be obtained as follows:

$$I_S = I_{L1} + I_{C1,on} = \frac{2}{1-D} I_o \tag{18}$$

The current that flows through the diodes D_1 and D_2 $(I_{D1}$ and $I_{D2})$ can be achieved as follows:

$$I_{D1} = I_{L2} + I_{C1,off} = \frac{1}{1-D} I_o \tag{19}$$

$$I_{D2} = I_{L1} - I_{C1,off} = \frac{1}{1-D} I_o \tag{20}$$

C. Discontinuous conduction mode

The operation modes in discontinuous conduction mode (DCM) can be divided into three modes. The first mode in (DCM) is the same as the first mode in (CCM). In the second mode, the diodes currents are decreasing and in the third mode the diodes D_1 and D_2 currents will be zero and the diodes and switch will turn off. The equivalent circuit and the typical waveform in third mode are shown in Figs. 4 and 5. In this mode, the inductors L_1 and L_2 currents will be constant; therefore, the voltage of the inductors L_1 and L_2 will be zero According to (19) and (20), the sum of the diodes D_1 and D_2 currents can be obtained as follows:

$$I_{D1} + I_{D2} = I_{L1} + I_{L2} \tag{21}$$

Using (19) and (20), the average currents of diodes D_1 and D_2 $(I_{D1,av}$ and $I_{D2,av})$ can be achieved as follows:

$$I_{D1,av} = I_{D2,av} = \frac{V_o}{R} \tag{22}$$

According to Fig. 5, the sum of the average current of diodes D_1 and D_2 during switching off period can be obtained as follows:

$$I_{D1,av} + I_{D2,av} = \frac{1}{2} \times D_{m2} \times I_{D-PK} \tag{23}$$

Where, D_{m2} is duty cycle in first mode at discontinuous conduction mode (DCM) and I_{D-PK} is sum of the peak currents of diodes D_1 and D_2 $\left(I_{D1-pk}\right.$ and $\left.I_{D2-pk}\right)$.

$$I_{D-pk} = I_{D1-pk} + I_{D2-pk} = \frac{V_i DT_s}{L_e} \tag{24}$$

Where,

$$\frac{1}{L_e} = \frac{1}{L_1} + \frac{1}{L_2} \tag{25}$$

By applying volt-sec balance principle on inductors L_1 and L_2, duty cycle in first mode at discontinuous conduction mode (D_{m2}) can be achieved as follows:

$$D_{m2} = \frac{2DV_i}{V_o} \tag{26}$$

Using (22)-(26), the voltage transfer gain in DCM $\left(M_{DCM}\right)$ can be earned as follows:

$$M_{DCM} = \frac{D}{\sqrt{\tau_L}} \tag{27}$$

Where, the parameter τ_L is defined as follows:

$$\tau_L = \frac{2L_e}{RT_s} \tag{28}$$

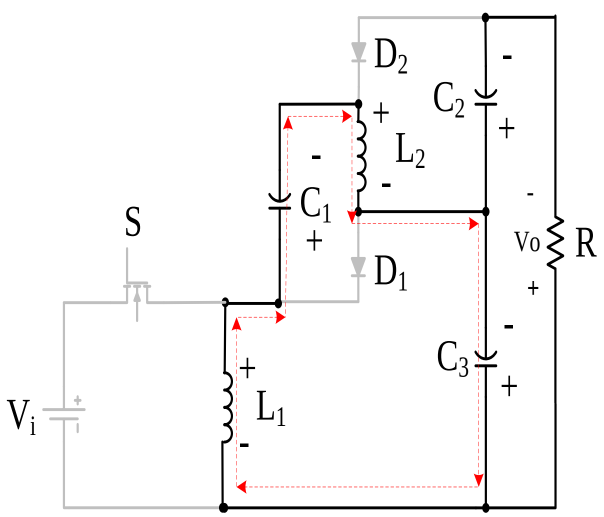

Fig. 4. Equivalent circuits of the presented converter in third mode at DCM operation

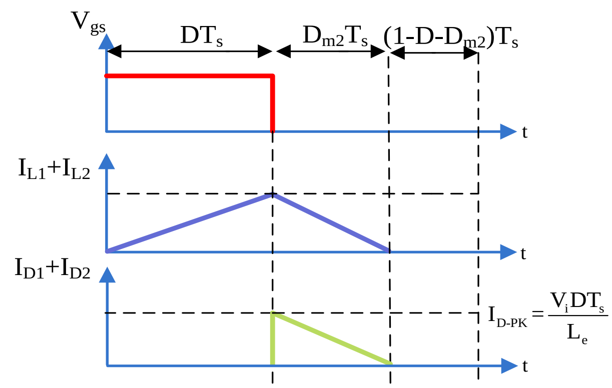

Fig. 5. Some illustrated waveforms of the proposed converter

D. Boundary condition mode

In this mode, the voltage transfer gain of the CCM is equal to the voltage transfer gain of the DCM. Using (9) and (27), the boundary normalized inductor time constant $\left(\tau_b\right)$ can be achieved as follows:

$$\tau_b = \frac{(1-D)^2}{4} \tag{29}$$

The relationship between the boundary normalized inductor time constant $\left(\tau_b\right)$ with different duty cycle is shown in Fig. 6. If τ_L is larger than τ_b, the proposed converter operates in continuous condition mode (CCM).

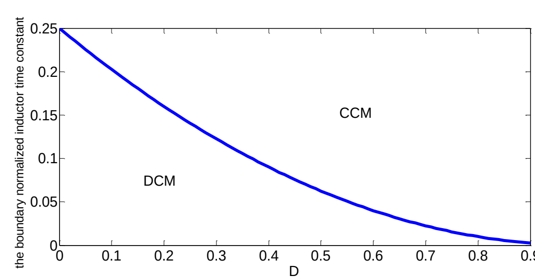

Fig. 6. Curves of voltage gain comparison of proposed converter and other converters at CCM operation

E. *Efficiency analysis*

For efficiency analysis of the proposed converter, parasitic resistance, the voltage ripple across the capacitors and the inductors is ignored.

The rms current of power switch S $\left(I_{S,rms}\right)$ can be achieved as follows:

$$I_{S,rms} = \sqrt{\frac{1}{T}\int_0^{DT_s} (I_{L1} + I_{C1,on})^2 dt} = \frac{2\sqrt{D}}{(1-D)} I_o \tag{30}$$

The power loss of switch S (P_{rDS}) can be calculated as follows:

$$P_{rDS} = r_{DS} I_{S,rms}{}^2 = \frac{4D}{(1-D)^2} I_o{}^2 \tag{31}$$

The rms current of diodes D_1 and D_2 $(I_{D1,rms}$ and $I_{D2,rms})$ can be obtained as follows:

$$I_{D1,rms} = I_{D2,rms} = \sqrt{\frac{1}{T_s} \int_{DT_s}^{T_s} \frac{I^2{}_o}{(1-D)^2} dt} = \frac{1}{\sqrt{1-D}} I_o \tag{32}$$

Forward resistance loss of diode D_1 $((P_{RF})_{D1})$ can be obtained as follows:

$$(P_{RF})_{D_1} = R_{F1} I^2{}_{D1,rms} = R_{F1} \frac{1}{1-D} I_o{}^2 \tag{33}$$

Forward voltage loss of diode D_1 $((P_{VF})_{D1})$ can be earned as follows:

$$(P_{VF})_{D1} = V_{F1} I_{D1,\text{av}} = V_{F_1} I_o \tag{34}$$

Forward resistance loss of diode D_2 $((P_{RF})_{D2})$ can be achieved as follows:

$$(P_{RF})_{D_2} = R_{F2} I_{D2,rms}{}^2 = R_{F2} \frac{1}{1-D} I_o{}^2 \tag{35}$$

Forward voltage loss of diode D_2 $((P_{VF})_{D2})$ can be obtained as follows:

$$(P_{VF})_{D2} = V_{F2} I_{D2,\text{av}} = V_{F2} I_o \tag{36}$$

The rms current of capacitors C_1 and C_2 $(I_{C1,rms}$ and $I_{C2,rms})$ can be obtained as follows:

$$\begin{aligned} I_{C1,rms} = I_{C2,rms} &= \sqrt{\frac{1}{T}\left[\int_0^{DT} (I_o)^2 dt + \int_{DT}^{T} \left(\frac{D}{1-D} I_o\right)^2 dt\right]} \\ &= \sqrt{\frac{D}{1-D}} I_o \end{aligned} \tag{37}$$

The power loss of capacitor C_1 (P_{RC1}) due to it ESR, can be achieved as follows:

$$P_{RC1} = r_{C1} I_{C1,rms}{}^2 = r_{C1} \frac{D}{1-D} I_o{}^2 \tag{38}$$

The power loss of capacitor C_2 (P_{RC2}) due to it ESR, can be calculated as follows:

$$P_{RC2} = r_{C2} I_{C2,rms}{}^2 = r_{C2} \frac{D}{1-D} I_o{}^2 \tag{39}$$

The rms current of capacitors C_3 $(I_{C3,rms})$ can be obtained as follows:

$$\begin{aligned} I_{C3,rms} &= \sqrt{\frac{1}{T}\left[\int_0^{DT} (2I_o)^2 dt + \int_{DT}^{T} \left(\frac{2D}{1-D} I_o\right)^2 dt\right]} \\ &= 2\sqrt{\frac{D}{1-D}} I_o \end{aligned} \tag{40}$$

The power loss of capacitors C_3 (P_{RC3}) can be expressed as follows:

$$P_{RC3} = r_{C3} I_{C3,rms}{}^2 = r_{C3} \frac{4D}{1-D} I_o{}^2 \tag{41}$$

The rms current of inductor L_1 $(I_{L1,rms})$ can be obtained as follows:

$$I_{L1,rms} = \frac{1+D}{1-D} I_o \tag{42}$$

The rms current of inductor L_2 $(I_{L2,rms})$ can be expressed as follows:

$$I_{L2,rms} = I_o \tag{43}$$

The conduction loss of inductor L_1 (P_{rL1}) can be obtained as follows:

$$P_{rL1} = R_{L1} \left(\frac{1+D}{1-D}\right)^2 I^2{}_o \tag{44}$$

The conduction loss of inductor L_2 (P_{rL2}) can be expressed as follows:

$$P_{rL2} = R_{L2} I^2{}_{L2,rms} = R_{L2} I_o{}^2 \tag{45}$$

Finally, the total power loss and efficiency of the proposed converter $(P_{loss}$ and $\eta)$ can be obtained as follows:

$$\begin{aligned} P_{loss} = P_{rDS} &+ \sum_{u=1}^{2} (P_{RF})_{Du} + \sum_{u=1}^{2} (P_{VF})_{Du} + \\ &\sum_{u=1}^{3} P_{RCu} + P_{rL1} + P_{rL2} \end{aligned} \tag{46}$$

$$\eta = \frac{P_o}{P_o + P_{loss}} = \frac{1}{1 + \frac{P_{loss}}{P_o}} \tag{47}$$

The voltage stress of the diodes D_1 and D_2 $(V_{D1}$ and $V_{D2})$ can be achieved as follows:

$$V_{D1} = V_{D2} = \frac{V_i}{1-D} \tag{48}$$

The voltage stress of the power switch S (V_S) can be obtained as follows:

$$V_S = \frac{V_i}{1-D} \tag{49}$$

The relationship between the normalized voltage stress across power switch of the proposed converter and other converters is depicted in Fig. 7. According to Fig. 7, the normalized voltage stress of the switch in the proposed converter is lesser than that in other converters.

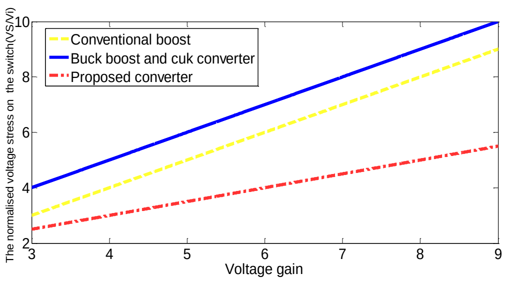

Fig. 7. Normalized switch voltage stress of the proposed converter versus voltage gain

E. Calculation of the voltage ripple of the capacitors

From Fig. 8, ΔV_{C1} can be achieved as foll

$$\Delta V_{C1} = \Delta V_{C1,ESR} + \Delta V_{C1,cap} \tag{50}$$

Also, $\Delta V_{C1,ESR}$ can be calculated as follows:

$$\Delta V_{C1,ESR} = ESR_{C1} \Delta I_{C1} \simeq ESR_{C1}(I_{C1,on} - I_{C1,off}) = \frac{ESR_{C1} I_o}{(1-D)} \tag{51}$$

Where, $$ESR_{C1} = \frac{\tan \delta_{C1}}{2\pi f_s} \tag{52}$$

$\Delta V_{C1,cap}$ can be achieved as follows:

$$\Delta V_{C1,cap} = \frac{I_{C1,on} DT_s}{C_1} = \frac{DT_s V_o}{RC_1} \tag{53}$$

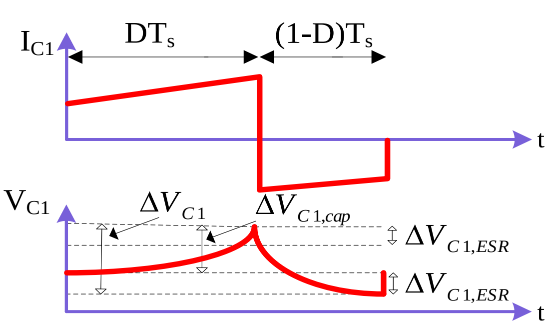

Fig. 8. The current and voltage of the capacitor C_1

From Fig. 9, ΔV_{C2} can be obtained as follows:

$$\Delta V_{C2} = \Delta V_{C2,ESR} + \Delta V_{C2,cap} \tag{54}$$

Also, $\Delta V_{C2,ESR}$ can be expressed as follows:

$$\Delta V_{C2,ESR} = ESR_{C2} \Delta I_{C2} \simeq ESR_{C2}(I_{C2,off} - I_{C2,on}) = \frac{ESR_{C2} I_o}{(1-D)} \tag{55}$$

Where,

$$ESR_{C2} = \frac{\tan \delta_{C2}}{2\pi f_s} \tag{56}$$

$\Delta V_{C2,cap}$ can be achieved as follows

$$\Delta V_{C2,cap} = \frac{I_{C2,off}(1-D)T_s}{C_2} = \frac{DT_s V_o}{RC_2} \tag{57}$$

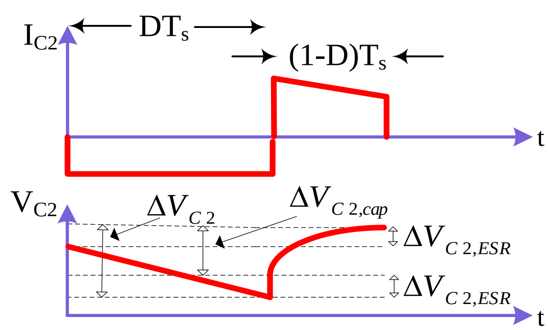

Fig. 9. The current and voltage of the capacitors C_2

From Fig. 10, ΔV_{C3} can be obtained as follows:

$$\Delta V_{C3} = \Delta V_{C3,ESR} + \Delta V \tag{58}$$

Also, $\Delta V_{C3,ESR}$ can be expressed as follows:

$$\Delta V_{C3,ESR} = ESR_{C3} \Delta I_{C3} \simeq ESR_{C3}(I_{C3,off} - I_{C3,on}) = \frac{2ESR_{C3} I_o}{(1-D)} \tag{59}$$

Where,

$$ESR_{C3} = \frac{\tan \delta_{C3}}{2\pi f_s} \tag{60}$$

$\Delta V_{C3,cap}$ can be achieved as follows:

$$\Delta V_{C3,cap} = \frac{I_{C3,off}(1-D)T_s}{C_3} = \frac{2DT_s V_o}{RC_3} \tag{61}$$

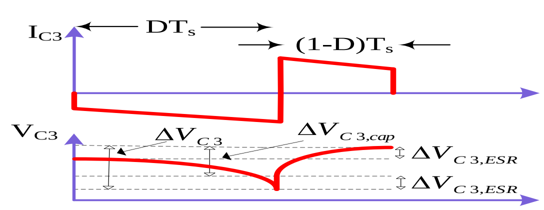

Fig. 10. The current and voltage of the capacitors C_3

The component normalized voltage and rms current stresses for the presented converter in CCM are shown in Table 1

TABLE I
THE COMPONENT NORMALIZED VOLTAGE AND RMS CURRENT STRESSES.

Circuit parameter	**Normalized voltage**	**Normalized rms current**
Switch S	$\frac{M_{CCM}+1}{2M_{CCM}}$	$\frac{\sqrt{M_{CCM}+2}}{\sqrt{M_{CCM}}}$
Capacitors C_1 and C_2	$\frac{1}{2}$	$\frac{1}{\sqrt{2M_{CCM}}}$
Capacitor C_3	$\frac{1}{2}$	$\frac{\sqrt{2}}{\sqrt{M_{CCM}}}$
Diodes D_1 and D_2	$\frac{M_{CCM}+1}{2M_{CCM}}$	$\frac{M_{CCM}+2}{\sqrt{2}M_{CCM}}$
Inductor L_1	-	$\frac{M_{CCM}+1}{M_{CCM}}$
Inductors L_2	-	$\frac{1}{M_{CCM}}$

In order to show the total device number and voltage gain of the proposed converter, conventional buck-boost and converters in ref 18-19, a comparison is made between the proposed topology and other converters. The device number and voltage gain of the structures are given in Table 2. As shown in Table 2, the proposed structure uses lower number of elements. and the total device of the other converters is higher comparing to their gains and voltage stresses. Based on the low voltage stress of the proposed converter, the efficiency of the proposed converter is higher comparing to its gain.

TABLE II
COMPARISON BETWEEN PROPOSED CONVERTER AND OTHER STRUCTURES

	Proposed converter	**Converter in 18**	**Converter in 19**		
Quantities of switches	1	1	3		
Quantities of diodes	2	2	3		
Quantities of capacitors	3	4	1		
Quantities of inductors	2	3	2		
Total device count	8	10	9		
Voltage stress of the switch	$\frac{V_o+2}{2}$	$\frac{V_o+2}{2}$	V_o	V_o	V_i
Voltage gain	$\frac{2D}{1-D}$	$\frac{2D}{1-D}$	$\frac{2D}{1-D}$		

E. Capacitor and inductor design

To confirm that the inductors L_1 and L_2 always work in CCM, the needed inductance values can be achieved as follows:

$$I_L \geq \frac{\Delta I_L}{2} \tag{62}$$

The minimum of inductors L_1, L_2 and L_3 to work in ccm operation mode can be achieved as follows:

$$\frac{1+D}{1-D} I_o \geq \frac{(1-D)V_o}{4L_1 f_s} \tag{63}$$

$$L_1 \geq \frac{V_o(1-D)^2}{4(1+D)I_o f_s} = \frac{42\times(1-0.48)^2}{4\times 2.6\times(1+0.48)\times 25\times 10^3} = 29\mu H \tag{64}$$

$$I_o \geq \frac{(1-D)V_o}{4L_{2,3} f_s} \tag{65}$$

$$L_2 \geq \frac{V_o(1-D)}{4I_o f_s} = \frac{42\times(1-.48)}{4\times 2.6\times 25\times 10^3} = 77\mu H \tag{66}$$

The minimum of the capacitors C_1, C_2 and C_3 can be obtained as follows:

$$C_{1,2} \geq \frac{DT_s V_o}{R\Delta V_{C1}} = \frac{DI_o}{0.01\times V_o \times f_s} = \frac{0.48\times 2.6}{0.02\times 42\times 25000} = 59\mu F \tag{67}$$

$$C_3 \geq \frac{I_{C3,off} T_s}{\Delta V_{C2,3}} = \frac{2DT_s V_o}{R\Delta V_{C2,3}} = \frac{2DI_o}{0.01\times V_o\times f_s} = \frac{2\times 0.48\times 2.6}{0.01\times 42\times 25000} = 118\mu F \tag{68}$$

III. EXPERIMENTAL RESULTS

To verify the operation of the proposed converter, the experimental results are provided. The specifications are as follows:

1) input voltage : 23 V
2) switching frequency: 25 kHz
3) switch: IRFP460A
4) switch on-state resistances: 0.03 ohm

5) diodes D_1 and D_2 : MUR860

6) diodes D_1 and D_2 forward resistances: 0.02 ohm

7) diodes D_1 and D_2 threshold voltages: 0.7 V

8) inductors L_1 : 83 µH

9) inductors L_2 : 245 µH

10) the equivalent series resistances (ESR) of inductor L_1 :0.012 ohm

11) the equivalent series resistances (ESR) of inductors L_2 :.020 ohm

12) capacitor C_1 and C_2 : 100 µF

13) capacitor C_3 : 470 µF

14) the equivalent series resistances (ESR)of capacitors C_1 and C_2 : 0.013 ohm

15) the equivalent series resistances (ESR)of capacitors $C_3\sqrt{b^2-4ac}$: 0.022 ohm

The proposed converter is operated in CCM operation mode. The output voltage waveform is shown in Fig. 11(a). The output voltage is equal to 42 V and the output power is 110 W. The inductors L_1 and L_2 currents waveforms are shown in Figs. 11(b), 11(c) respectively. According to (14) and (16), the average values of inductors L_1 and L_2 currents are equal to 7.4 and 2.6 A, respectively, which closely agree with the experimental results. The voltages of diodes D_1 and D_2 waveforms is shown in Fig. 11(d). According to (48), the voltage across diodes D_1 and D_2 is equal to 44 V, which is equal to experimental results. The voltages of switch waveform is shown in Fig 11(e). According to (49), the voltage across switch S is equal to 44 V, that is verified by the obtained value from experimental results. The current that flows through the diodes D_1 and D_2 is shown in Fig. 11(f). According to (19) and (20), the average value of diodes D_1 and D_2 currents is equal to 6.5 A, which closely agree with experimental results The switch S current waveform is shown in Fig. 11(g). According to (18), the average value of switch S current is equal to 13 A, which closely agree with the experimental results. From Fig. 12, the measured efficiency of the proposed converter is 92.6% at the full-load condition and the maximum efficiency is 95.1%.

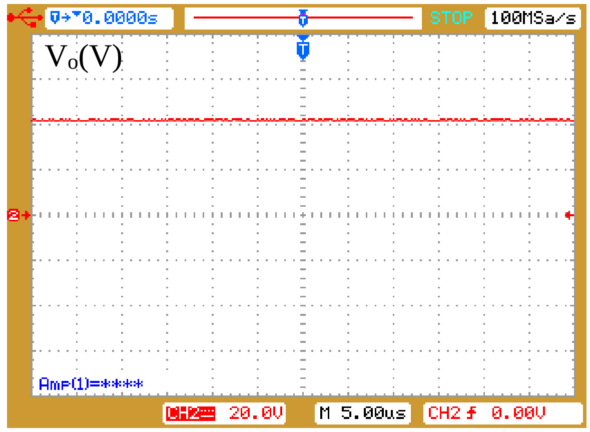

(a) Output voltage

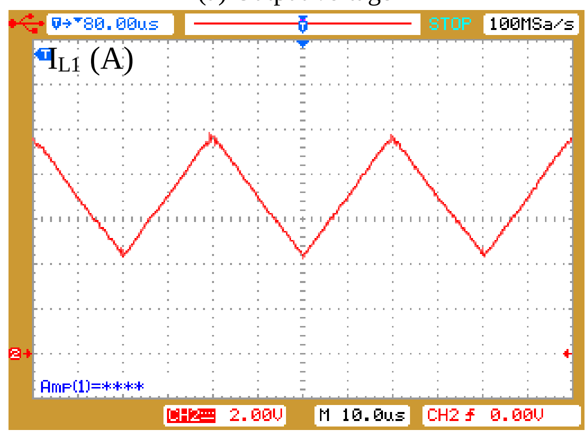

(b) Inductor L_1 current

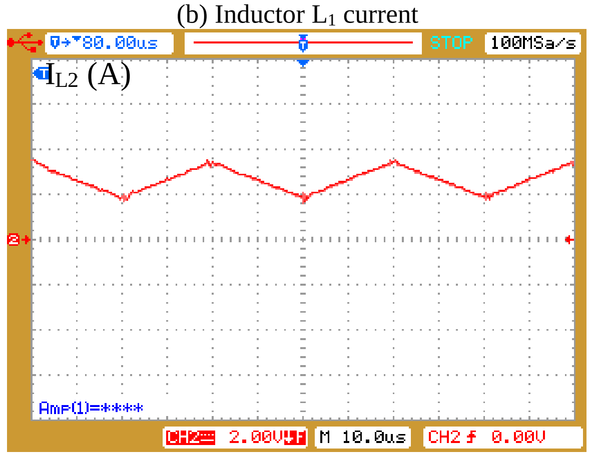

(c) Inductor L_2 current

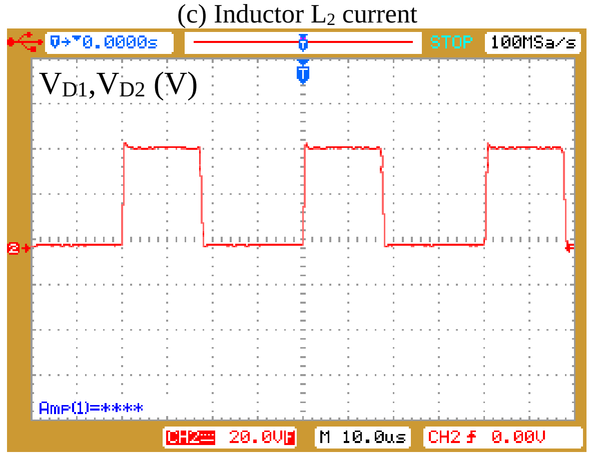

(d) Diodes D_1 and D_2 voltage

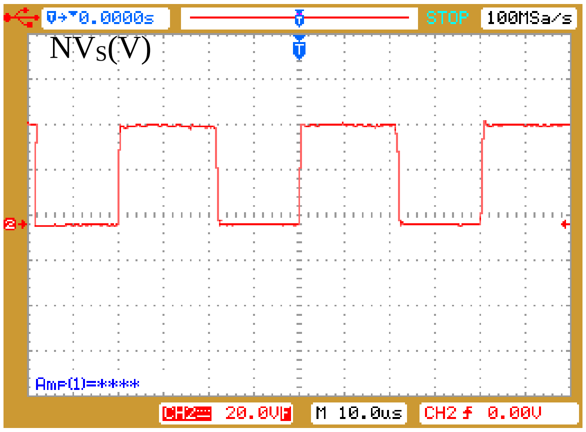

(e) Switch S voltage

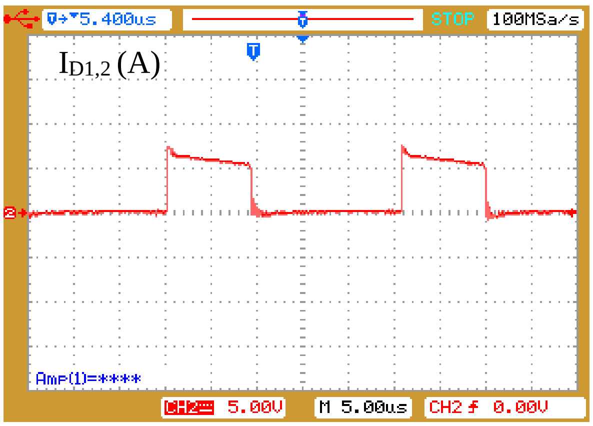

(f) Diodes D_1 and D_2 current

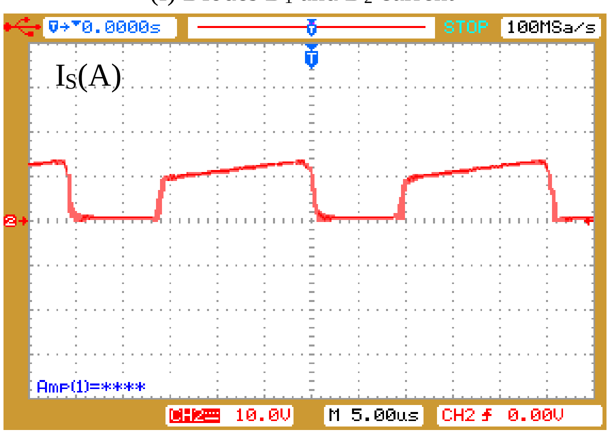

(g) Switch S current

Fig. 11. Experimental results

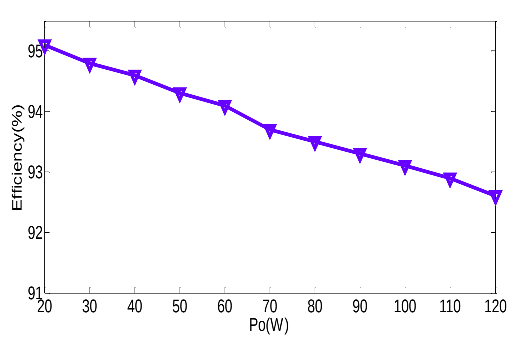

Fig. 12. Measured efficiency of the proposed converter

IV. CONCLUSION

In this paper, a novel transformer less buck boost dc-dc converter is presented. The output voltage of some sources such as fuel cell, photovoltaic and battery based systems are not regulated. Therefore voltage regulation is required to fix the DC-link voltage. Hence, a buck boost DC/DC converter is suitable to regulate the output voltage of these sources The structure of the presented buck-boost converter is simple. In the proposed converter, only one main switch is utilized, which decreases the conduction loss of power switch and improves efficiency. The voltage stress across the power switch is low and switch with low on-state resistance can be selected. The step-up voltage gain of the proposed buck-boost converter is higher than that of the classic boost, buck-boost ,CUK, SEPIC and ZETA converters. The proposed converter has simple structure; therefore, the control of the presented converter will be easy. The buck-boost converters is utilized in many applications like gadgets such as mobile phones and notebooks, fuel-cell systems, car electronic devices and LED drivers. Finally, the experimental results are provided to verify the feasibility of the proposed converter.

REFERENCES

[1] K. Jin, X. Ruan, M. Yang, and M. Xu, “A hybrid fuel cell power system,” IEEE Trans. Ind. Electron., vol. 56, pp. 1212–1222, 2009.

[2] W. S. Liu, J. F. Chen, T. J. Liang, R. L. Lin, and C. H. Liu, “Analysis, design, and control of bidirectional cascoded configuration for a fuel cell hybrid power system,” IEEE Trans. Power Electron., vol. 25, pp. 1565–1575, 2010.

[3] S.-K. Changchien, T.-J. Liang, J.-F. Chen, and L.-S. Yang, “Novel high step-up DC-DC converter for fuel cell energy conversion system,” IEEE Trans. Ind. Electron., vol. 57, pp. 2007-2017, 2010.

[4] W. Jiang and B. Fahimi, “Active current sharing and source management in fuel cell-battery hybrid power system", IEEE Trans. Ind. Electron. , vol. 57, pp. 752 -76, 2010.

[5] Q. Haibo, Z. Yicheng, Y. Yongtao and W. Li, “Analysis of buck-boost converters for fuel cell electric vehicles", in Proc. IEEE Int. Conf. Veh. Electron. Safety, pp. 109 -113, 2006.

[6] R. J. Wai, C. Y. Lin, R. Y. Duan, and Y. R. Chang, “High-efficiency DC–DC converter with high voltage gain and reduced switch stress,” IEEE Trans. Ind. Electron., vol. 54, pp. 354–364, 2007.

[7] T. J. Liang, J. H. Lee, S. M. Chen, J. F. Chen, L. S. Yang, “Novel Isolated High-Step-Up DC–DC Converter With Voltage Lift,” IEEE Trans. Ind. Electron., vol. 60, pp. 1483-1491, 2013.

[8] G. Spiazzi, P. Mattavelli, A. Costabeber, “Effect of Parasitic Components in the Integrated Boost-Flyback High Step-Up Converter,” IECON '09. 35th Annual Conference of IEEE, pp. 420 – 425, 2009.

[9] H. C. Shu, “Design and analysis of a switched-capacitor-based step-up dc/dc converter with continuous input current,” IEEE Trans. Circuits Syst. I, Fundam. Theory Appl., vol. 46, pp. 722–730, 1999.

[10] Y. P. Hsieh, J. F. Chen, T. J. Liang, and L. S. Yang, “Novel high step-up DC–DC converter with coupled-inductor and switched-capacitor techniques,” IEEE Trans. Ind. Electron., vol. 59, pp. 998–1007, 2012.

[11] O. Abutbul, A. Gherlitz, Y. Berkovich and A. Ioinovici, “Step-up switching-mode converter with high voltage gain using a switched-capacitor circuit.” IEEE Trans. Circuits Syst. I, vol. 50, pp. 1098-1102, 2003.

[12] K. I. Hwu and W.Z. Jiang, “Isolated step-up converter based on flyback converter and charge pumps,” IET Power Electron., vol. 7, pp. 2250–2257, 2014.

[13] S. M. Chen, T. J. Liang, L. S. Yang, and J. F. Chen, “A boost converter with multiplier and coupled inductor for AC module applications,” IEEE Trans. Ind. Electron., vol. 60, pp. 1503–1511, 2013.

[14] S. C. Tan, M. Nur, S. Kiratipongvoot, S. Bronstein, Y. M. Lai, C. K. Tse, and A. Ioinovici, “Switched-capacitor converter configuration with low EMI emission obtained by interleaving and its large-signal modeling,” in Proc. IEEE Int. Symp. Circuits Syst., pp. 1081-1084, 2009

[15] Y. P. Hsieh, J. F. Chen, L. S. Yang, C. Y. Wu and W. S. Liu, “High-Conversion-Ratio Bidirectional DC–DC Converter With Coupled Inductor,” IEEE Trans. Ind. Electron., vol. 61, pp. 210-222, 2014.
[16] L. S. Yang, T. J. Liang, and J. F. Chen, “Transformer-less DC–DC converter with high voltage gain,” IEEE Trans. Ind. Electron., vol. 56, pp. 3144–3152, 2009.
[17] Al-Saffar, M.A.; Ismail, E.H., A high voltage ratio and low stress DC-DC converter with reduced input current ripple for fuel cell source,” Renewable Energy, 2015
[18] M. R. Banaei, H. Ardi and A. Farakhor, “Analysis and implementation of a new single-switch buck–boost DC/DC converter,” IET Power Electron., vol. 7, pp. 1906–1914, 2014.
[19] H. K. Liao, T. J. Liang, L. S. Yang and J. F. Chen, “Non-inverting buck–boost converter with interleaved technique for fuel-cell system”, IET Power Electron., vol. 5, pp. 1379-1388, 2012.
[20] C. T. Pan, C. F. Chuang and C. C. Chu, “A novel transformerless interleaved high step-down conversion ratio DC-DC converter with low switch voltage stress”, IEEE Trans. Ind. Electron., vol. 61 , pp. 5290 - 5299, 2014
[21] K. I. Hwu and T. J. Peng, “A novel buck boost converter combining KY and buck converters,” IEEE Trans. Power Electron., vol. 27, pp. 2236 - 2241, 2012.
[22] A. A. Boora, F. Zare, and A. Ghosh, “Multi-output buck-boost converter with enhanced dynamic response to load and input voltage changes,” IET Power Electronics, vol. 4, pp. 194-208, 2011.
[23] T.-J. Liang and J.-H. Lee, “double-deck buck-boost converter with soft switching operation,” IEEE Trans. Power.Electron., vol. 31, pp. 4324 - 4330, 2016.
[24] M. He, F. Zhang, J. Xu, P. Yang and T. Yan, "High-efficiency two-switch tri-state buck-boost power factor correction converter with fast dynamic response and low-inductor current ripple,” IET Power Electronics., vol. 6, pp. 1544-1554, 2013.
[25] Rong-Jong Wai; Chung-You Lin; Bo-Han Chen, “High-Efficiency DC–DC Converter With Two Input Power Sources,” IEEE Trans. Power Electron., vol. 27, pp. 1862-1875, 2012.
[26] Zhan Wang; Hui Li, “An Integrated Three-Port Bidirectional DC–DC Converter for PV Application on a DC Distribution System,” IEEE Trans. Power Electron., vol. 28, pp. 4612-4624, 2013.
[27] H. Liao , T. Liang , L. Yang and J. Chen, “Non inverting buck-boost converter with interleaved technique for fuel-cell system,” IET Power Electron., vol. 5, pp. 1379-1388, 2012
[28] K. I. Hwu, and W. Z. Jiang, “Voltage Gain Enhancement for a Step-Up Converter Constructed by
[29] KY and Buck-Boost Converters,” IEEE Trans. Ind. Electron., vol. 61, pp. 1758–1768, 2014.
[30] K. Filsoof, A. A. Hagar and P. Lehn, “A transformerless modular step-up dc-dc converter for high power applications,” IET Power Electronics., vol. 7, pp. 2190-2199, 2014
[31] R. Hosoki, H. Koizumi, “High-step-up dc–dc converter using voltage multiplier cell with ripple free input current,” IEEE IECON’13., pp. 834–839, 2013.
[32] Sathyan, S., Suryawanshi, H.M, “Interleaved high step-up converter for renewable energy sources,” IEEE IECON’13., pp. 918–923, 2013
[33] Lung-Sheng Yang, Tsorng-Ju Liang, Jiann-Fuh Chen. “Transformerless DC–DC Converters With High Step-Up Voltage Gain,” IEEE Trans. Ind. Electron., vol. 56, pp. 3144-3152, 2009